

Test of relativistic time dilation with fast optical atomic clocks at different velocities

SASCHA REINHARDT¹, GUIDO SAATHOFF¹, HENRIK BUHR¹, LARS A. CARLSON¹, ANDREAS WOLF¹, DIRK SCHWALM¹, SERGEI KARPUK², CHRISTIAN NOVOTNY², GERHARD HUBER², MARCUS ZIMMERMANN³, RONALD HOLZWARTH³, THOMAS UDEM³, THEODOR W. HÄNSCH³ AND GERALD GWINNER^{4*}

¹Max-Planck-Institut für Kernphysik, 69029 Heidelberg, Germany

²Institut für Physik, Universität Mainz, 55099 Mainz, Germany

³Max-Planck-Institut für Quantenoptik, 85748 Garching, Germany

⁴Dept. of Physics & Astronomy, University of Manitoba, Winnipeg R3T 2N2, Canada

*e-mail: gwinner@physics.umanitoba.ca

Published online: 11 November 2007; doi:10.1038/nphys778

Time dilation is one of the most fascinating aspects of special relativity as it abolishes the notion of absolute time. It was first observed experimentally by Ives and Stilwell in 1938 using the Doppler effect. Here we report on a method, based on fast optical atomic clocks with large, but different Lorentz boosts, that tests relativistic time dilation with unprecedented precision. The approach combines ion storage and cooling with optical frequency counting using a frequency comb. ⁷Li⁺ ions are prepared at 6.4% and 3.0% of the speed of light in a storage ring, and their time is read with an accuracy of 2×10^{-10} using laser saturation spectroscopy. The comparison of the Doppler shifts yields a time dilation measurement represented by a Mansouri–Sexl parameter $|\hat{\alpha}| \leq 8.4 \times 10^{-8}$, consistent with special relativity. This constrains the existence of a preferred cosmological reference frame and CPT- and Lorentz-violating ‘new’ physics beyond the standard model.

Since its introduction by Albert Einstein in 1905 (ref. 1), special relativity has been the accepted theory of local space-time. It not only resolved severe open questions in electrodynamics but introduced a revolutionary new notion of space and time that influenced a variety of areas from technology² to philosophy³. Today its main ingredient, the space-time symmetry of local Lorentz invariance, is deeply woven into all physical theories describing nature on a fundamental level: the standard model of particle physics is based on relativistic quantum field theories, and the theory of general relativity contains local Lorentz invariance in the limiting case of negligible gravitation. This symmetry is therefore one of the pillars of today’s description of all four known fundamental forces. Already this prominent role alone demands thorough empirical affirmation, and further motivation for experimental tests comes from a variety of unsettled problems in contemporary physics. For example, one possible explanation of the abundance of matter versus antimatter is the violation of charge-conjugation, parity, time-reversal (CPT) symmetry, which is closely related to local Lorentz symmetry^{4,5}. In string theory and also in the quest for a quantum theory of gravity, which unifies the standard model of particle physics with general relativity in a ‘theory of everything’, Lorentz violation is frequently assumed^{6–8} and could thus provide a distinctive experimental signature for new physics.

Time dilation was proposed as an experimental test by Einstein in 1907 (ref. 9). The idea was to measure the Doppler shift of light emitted from moving particles. Einstein showed that time dilation leads to the ether-independent relativistic Doppler formula

$\nu_0 = \nu_l \gamma (1 - \beta \cos \theta)$. Here, ν_l and ν_0 denote the frequencies in the laboratory reference frame of the observer and the particles’ rest frame moving at velocity $v = \beta c$ with respect to the observer, respectively, θ is the angle of observation with respect to the particles’ movement as measured in the laboratory frame and $\gamma = 1/\sqrt{1 - v^2/c^2}$. The first time dilation measurement was carried out by Ives and Stilwell in 1938 (ref. 10). They used a collinear set-up in which the Doppler-shifted frequencies of light emitted from hydrogen canal rays were measured both in forward and backward directions relative to the atomic motion. For the simultaneous measurement of the Doppler-shifted frequencies $\nu_p = \nu_0/\gamma(1 - \beta)$ parallel and $\nu_a = \nu_0/\gamma(1 + \beta)$ antiparallel to the particles’ motion in the laboratory frame, the $\beta \cos \theta$ terms are cancelled by the time dilation factors in the product of these Doppler shifts, yielding

$$\nu_0^2 = \nu_a \nu_p, \quad (1)$$

assuming plane waves. The β -independence of this relation is a consequence of time dilation in special relativity and therefore of the relativity principle, and the outcome of the Ives–Stilwell experiment is independent of the chosen clock synchronization scheme¹¹.

Various test theories have been developed to describe possible deviations from special relativity¹². For the purpose of quantifying our experimental results, we adopt the one by Robertson¹³, Mansouri and Sexl¹⁴ (RMS), which is widely used to compare different experiments. In this model, Einstein’s postulates are abandoned and general linear transformations between a

hypothetical preferred reference frame $\Sigma(T, \mathbf{X})$ and a frame $S(t, \mathbf{x})$ moving at a velocity V along X with respect to Σ are derived, assuming an isotropic speed of light c only for the preferred frame. Using Einstein synchronization, these generalized Lorentz transformations read:

$$T = \Gamma \left(\frac{t}{\hat{a}} + \frac{Vx}{\hat{b}c^2} \right);$$

$$X = \Gamma \left(\frac{x}{\hat{b}} + \frac{Vt}{\hat{a}} \right); \quad Y = \frac{y}{\hat{d}}; \quad Z = \frac{z}{\hat{d}},$$

with $\Gamma = (1 - V^2/c^2)^{-1/2}$. The three velocity-dependent test functions $\hat{a}(V^2)$, $\hat{b}(V^2)$ and $\hat{d}(V^2)$ parameterize time dilation as well as Lorentz contraction in the longitudinal and transverse directions. For special relativity, they are all unity. By expanding these functions in powers of V^2/c^2 , that is, $\hat{a}(V^2) = [1 + \hat{\alpha}V^2/c^2 + \mathcal{O}(c^{-4})]$ and so on, three test parameters $\hat{\alpha}$, $\hat{\beta}$ and $\hat{\delta}$ are obtained. The Ives–Stilwell experiment tests $\hat{\alpha}$, Michelson–Morley tests $|\hat{\beta} - \hat{\delta}|$ (ref. 15) and Kennedy–Thorndike tests $|\hat{\alpha} - \hat{\beta}|$ (ref. 16). An analysis of Doppler shift experiments within the RMS test theory has been carried out^{17,18} and shows that a non-vanishing $\hat{\alpha}$ would modify the outcome of the Ives–Stilwell experiment as

$$\frac{v_p v_a}{v_0^2} = 1 + 2\hat{\alpha}(\beta^2 + 2\beta_{\text{lab}} \cdot \boldsymbol{\beta}) + \mathcal{O}(c^{-4}), \quad (2)$$

with $\boldsymbol{\beta}_{\text{lab}} = \mathbf{V}_{\text{lab}}/c$. The β^2 term used in our experiment allows us to determine $\hat{\alpha}$ absolutely without having to rely on the precise knowledge of β_{lab} (for $\beta \gg \beta_{\text{lab}}$). The $2\boldsymbol{\beta}_{\text{lab}} \cdot \boldsymbol{\beta}$ term used by most other experiments gives access to $\hat{\alpha}$ via sidereal modulations, but makes the interpretation dependent on Σ , which is generally assumed to be the cosmic-microwave-background rest frame ($|\mathbf{V}_{\text{lab}}| \approx 350 \text{ km s}^{-1}$). A sidereal analysis using the $2\boldsymbol{\beta}_{\text{lab}} \cdot \boldsymbol{\beta}$ term is feasible and in progress. However, we do not expect it to reach the sensitivity derived from the β^2 term presented here, mainly because $\beta \approx 55\beta_{\text{lab}}$.

It should be stressed at this point that our experiment is sensitive to any deviation from special relativity that affects time dilation and does not depend on the assumption of a preferred reference frame. There are other approaches such as doubly special relativity¹⁹, characterized by two observer-independent scales (velocity c and Planck momentum/length), where time dilation is modified without invoking preferred frames, but for which the effects on Doppler experiments have not yet been worked out explicitly.

The original Ives–Stilwell experiment confirmed time dilation as predicted by special relativity to about 1%. Three technical developments have led to major improvements: (1) high-resolution laser spectroscopy starting in the 1970s leading to limits on $\hat{\alpha}$ in the 10^{-6} range^{20–22}, (2) modern ion beam storage and cooling, and (3) frequency counting in the optical domain, the latter two being reported here.

In our experiment at the Max Planck Institute for Nuclear Physics, ${}^7\text{Li}^+$ ions are accelerated by a tandem Van de Graaff accelerator and injected into the test storage ring (TSR) shown in Fig. 1. The helium-like ${}^7\text{Li}^+$ exhibits the strong $2s\ ^3S_1(F=5/2) \rightarrow 2p\ ^3P_2(F=7/2)$ two-level transition at 548 nm in its metastable triplet spectrum. The 50 s vacuum lifetime of the metastable ground state $2s\ ^3S_1$ is quenched to 10–20 s owing to collisions with the rest gas, still sufficiently long to carry out laser spectroscopy. To extract time dilation from a measurement of the Doppler shifts at one ion velocity, the rest-frame transition frequency needs to be known accurately. Riis *et al.*²³ measured it

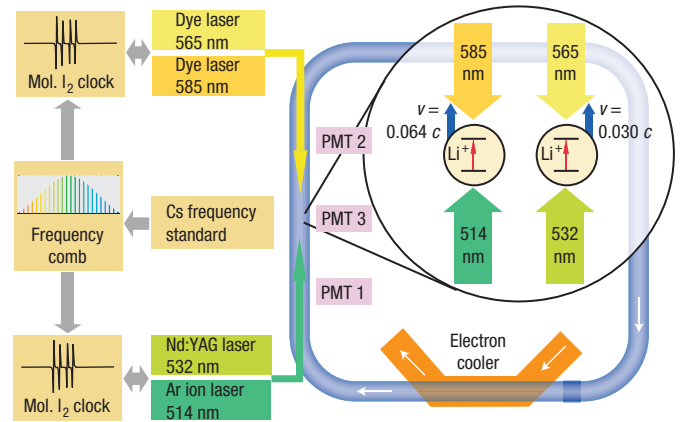


Figure 1 Schematic diagram of the TSR. Li^+ ions circulate in the 55-m-circumference ring. In the electron cooler, cold electrons are overlapped with the ions and provide cooling. The measurements at the two different velocities are carried out sequentially. In the experiment, the two lasers are coupled into the ring from the same side and are retro-reflected.

with an uncertainty of 400 kHz, which was the limiting factor in our previous time dilation measurement²⁴. Moreover, another rest-frequency measurement exists²⁵ that differs from that of ref. 23 by more than 2σ . To overcome this limitation, and to carefully study and characterize numerous systematic effects that emerge at the 100 kHz level such as laser forces on the ions and magnetic stray fields, we decided to set up a new experiment that fully exploits the superb ion beam quality at the TSR by measuring the same transition at two different velocities. In the TSR, ${}^7\text{Li}^+$ can be stored at velocities ranging from $\beta_1 \approx 0.030$ to $\beta_2 \approx 0.064$. The Doppler-shifted frequencies $\nu_a^{(1,2)}$ and $\nu_p^{(1,2)}$ measured at β_1 and β_2 can be combined using equation (2) (neglecting the sidereal term) to

$$\frac{\nu_a^{(2)} \nu_p^{(2)}}{\nu_a^{(1)} \nu_p^{(1)}} = \frac{1 + 2\hat{\alpha}\beta_2^2}{1 + 2\hat{\alpha}\beta_1^2} \approx 1 + 2\hat{\alpha}(\beta_2^2 - \beta_1^2), \quad (3)$$

independent of the rest-frame frequency. As $\beta_2^2 - \beta_1^2 \approx 0.8\beta_2^2$, the sensitivity is not significantly diminished.

The moving clocks are read using laser saturation spectroscopy. The laboratory frequencies ν_p and ν_a of the parallel and antiparallel laser beams (with respect to the ion beam) must obey relation (2) for resonance, which is indicated by a dip in the fluorescence spectrum. Through permanent cooling of the ions by a cold electron beam, the ion beam's width shrinks to $\approx 250 \mu\text{m}$, the divergence to $\approx 50 \mu\text{rad}$ and the longitudinal momentum spread to $\delta p/p = 3.5 \times 10^{-5}$, leading to a Doppler width of the transition of about 2.5 GHz full-width at half-maximum. This broadening is overcome in saturation spectroscopy by selecting a narrow velocity class of the order of the natural linewidth; two lasers are overlapped parallel and antiparallel with the ion beam, respectively, and excite the clock transition. With both laser intensities equal and of the order of 6.7 mW cm^{-2} (saturation intensity I_s), the fluorescence yields get saturated, that is, they become almost independent of the intensity, whereas at low intensity they increase linearly. In this saturation regime, each ion contributes nearly the same amount of fluorescence when exposed to one or both lasers. In general, the lasers interact with ions of two different velocity classes which then both contribute separately to the total fluorescence. However, in the case where equation (2) holds, both lasers are resonant with the same velocity class β and the number of fluorescing ions is reduced

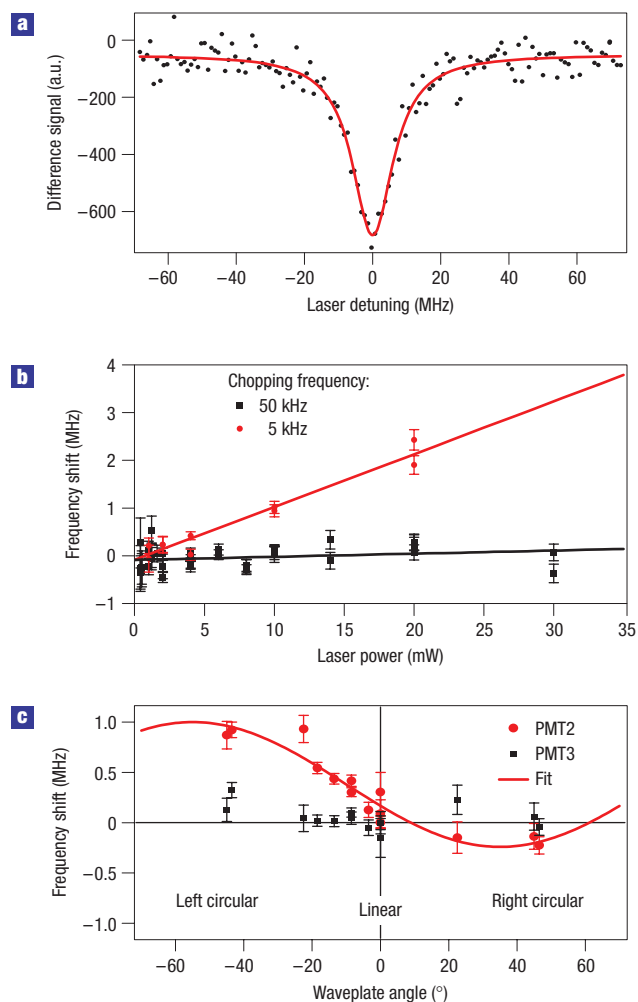


Figure 2 Results from the saturation spectroscopy. All error bars represent statistical 1σ errors obtained from fitting the Lamb dip. **a**, Lamb dip after background subtraction and fitted by a Lorentzian. **b**, Lamb-dip centre frequency versus laser power for chopping frequencies of 5 and 50 kHz. **c**, Lamb-dip frequencies measured at two different positions versus degree of polarization.

by half. The corresponding decrease of the total fluorescence is referred to as the Lamb dip. The co-propagating laser (a Nd:YAG laser at 532 nm for β_1 and an argon-ion laser at 514 nm for β_2) is fixed in frequency by locking it to a well-known iodine (I_2) line, whereas the counter-propagating light is generated by a tunable dye laser (at 565 nm and 585 nm for β_1 and β_2 , respectively). The dye laser frequency is referenced to a second, I_2 -stabilized dye laser by a tunable frequency-offset lock. All I_2 locks are implemented by frequency-modulated saturation spectroscopy. The iodine lines for the dye laser are calibrated using an optical frequency comb^{26,27}. All laser frequencies are known absolutely to 70 kHz during the whole experiment.

The mean velocity of the ion beam is adjusted for the fixed-frequency laser at $v_p^{(1,2)}$ to select ions in the centre of the velocity distribution. The dye laser is scanned around $v_a^{(1,2)}$ and the Lamb dip in the fluorescence is recorded with photomultipliers (PMTs) from the side; its frequency is measured with respect to the I_2 clock in the laboratory frame. As shown in Fig. 1, the lasers overlap with the ion beam for a short distance in the bending magnet where the clock transition is shifted owing to the strong

magnetic fields and the curved trajectories of the ions. However, the fluorescence from this region has sufficiently decayed away once the ions reach the detectors. The laser beams are merged with a dichroic mirror and guided to the TSR by a single-mode fibre; they are linearly polarized in the same direction, and their intensities are adjusted to balance the laser forces on the ions. The beams leaving the fibre are expanded in a telescope, sent through the TSR, retro-reflected by a flat mirror and coupled back into the fibre. They are accurately overlapped with the ion beam using computer-controlled motorized translation/rotation stages. By simultaneously maximizing the fluorescence yield recorded with three PMTs located at different positions along the beam pipe, the dye laser beam and the ion beam are aligned to better than $70\ \mu\text{rad}$, limiting line shifts due to angular misalignment to less than 50 kHz at β_2 . The ion beam divergence adds less than 50 kHz.

After each ion injection into the TSR, the lasers are switched off for the first 7 s until the ion beam is cooled with electrons to equilibrium. Then, the lasers are turned on and the fluorescence rate is recorded as a function of the dye laser frequency as shown in Fig. 2a. As the limited lifetime of the metastable ions in the TSR leads to a decrease of the fluorescence during a laser scan, the latter is kept asynchronous with the injection cycle. After adding a sufficiently large number of scans, the ion beam decay averages out. To remove distortions of the fluorescence signal caused by laser power fluctuations and varying ion currents between injections, the Doppler-broadened background is measured quasi-simultaneously with the Lamb dip by fast switching between three different laser beam configurations and recording the fluorescence as three separate spectra. The lasers are chopped with acousto-optic modulators at a rate of 5 to 200 kHz. One spectrum, taken with both lasers on, contains the Doppler-broadened background and the Lamb dip. The other two are recorded with the lasers applied separately, the sum of which reflects the Doppler background alone. Subtracting them leads to the Lamb-dip spectrum shown in Fig. 2a. As one laser is fixed in frequency, the resonance is twice as wide as in standard saturation spectroscopy, where both beams are tuned. The Lamb dip shown is recorded at a laser power of 1.13 mW, which corresponds to $\approx 1.5 I_s$. The observed resonance widths are in accordance with the natural linewidth of the $2^3S \rightarrow 2^3P$ transition of 3.7 MHz (that is, a resonance width of 7.4 MHz), once the broadening mechanisms present in our experiment are accounted for. Broadening is mainly caused by saturation, but also by the finite spectral widths of the lasers, and the finite exposure time of the ions to the laser light (time-of-flight broadening). The narrowest observed resonance is 10.8 MHz wide, at an intensity of $\approx 0.6 I_s$.

In Fig. 2b, the Lamb-dip centre frequency $\delta\nu$ is plotted versus the total laser intensity. At 5 kHz switching frequency, an intensity dependence is apparent, attributed to local changes in the velocity distribution caused by the laser forces. They modify the Doppler-broadened background and distort the Lamb dip. Only distortions that build up on a timescale longer than the laser switching time of 200 μs are cancelled by the subtraction scheme. We find that switching at 50 kHz largely eliminates this effect. The fit uncertainty is about 100 kHz and the extrapolated Lamb-dip frequencies for 50 kHz and 5 kHz coincide at this level. To estimate the uncertainty of this effect, we apply the model by Artoni *et al.*²⁸ as a worst-case scenario, from which we estimate shifts of (149 ± 72) kHz for the $\beta_1 = 0.030$ experiment and (47 ± 23) kHz at $\beta_2 = 0.064$.

Linearly polarized light minimizes frequency shifts due to magnetic stray fields. For an unpolarized ion beam, first-order Zeeman shifts average out. However, at the 100 kHz level, optical pumping together with the Zeeman effect may cause shifts. Figure 2c shows the measured Lamb-dip position as a function of the laser polarization. The sinusoidal polarization dependence indicates fields of around 1 G at PMT2, but less than 0.2 G at PMT3,

which is farther from the TSR magnets. The shifted base line of the sine at PMT2 is probably due to ion beam polarization caused by optical pumping. For linear polarization, the magnetic field and the beam polarization lead to an uncertainty of the Lamb-dip position of only 50 kHz at PMT3.

A further influence on the Lamb-dip frequency is caused by the gaussian phase structure of the laser beams, which shows a phase deviation (Gouy phase shift) $\xi(z) = \arctan(z/z_R)$ from a plane wave in the direction of the optical axis z , where z_R denotes the Rayleigh range and $z = 0$ the focal point. For a particle travelling along z at velocity v , this phase change results in a frequency shift of $\delta\nu^{wf} = \gamma v d\xi(z)/dz$. However, if the two counter-propagating beams are phase-matched, their Gouy phase shifts compensate each other. This is achieved by putting the foci on the flat retro-reflecting mirror. Residual shifts due to the imperfect placement of the foci are determined by carefully measuring the beam profiles of both lasers frequently during the beam times (a typical value for the Rayleigh range is 4 m). A Monte Carlo simulation based on these measurements estimates shifts of up to 60 kHz for β_2 and 40 kHz for β_1 , which are corrected for.

Taking all systematic errors into account, the transition frequencies ν_a and ν_p measured at $\beta_1 = 0.030$ and $\beta_2 = 0.064$ yield special-relativity values for the rest-frame frequency (equation (1)) of

$$\sqrt{\nu_a^{(1)} \nu_p^{(1)}} = (546\,466\,918\,577 \pm 108) \text{ kHz} \quad \text{and}$$

$$\sqrt{\nu_a^{(2)} \nu_p^{(2)}} = (546\,466\,918\,493 \pm 98) \text{ kHz},$$

respectively. From equation (3) follows a test parameter

$$\hat{\alpha} = (-4.8 \pm 8.4) \times 10^{-8},$$

which is consistent with special relativity. The new upper limit of $|\hat{\alpha}| \leq 8.4 \times 10^{-8}$ is more than an order of magnitude smaller than that obtained from non-storage-ring experiments^{29,30}. Our previous limit based on a measurement at β_2 only²⁴ is tightened by nearly a factor of three. More importantly, its dependence on the ${}^7\text{Li}^+$ rest-frame frequency measurements is overcome. In addition, assuming that Lorentz invariance holds (that is, $\hat{\alpha} = 0$), we can also derive a rest frequency for the $2s\,{}^3S_1(F=5/2) \rightarrow 2p\,{}^3P_2(F=7/2)$ transition in ${}^7\text{Li}^+$ of $(546\,466\,918\,531 \pm 73)$ kHz, in agreement with ref. 23, but five times more precise. This aspect is valuable for an improved determination of the Li^+ Lamb shift.

The dual-boost method introduced with this experiment can open up laser-spectroscopic time dilation measurements at much higher γ at large storage rings. In this domain, the limited wavelength range where narrow-band lasers are available will make it difficult if not impossible to measure Doppler-shifted and rest frequencies of a transition in a highly charged ion with the required precision. Using resonant two-photon spectroscopy with highly asymmetric excitation frequencies in the rest frame (for example, one in the extreme-ultraviolet, the other in the far-infrared region), it might be possible to find two boosts that shift both excitation steps simultaneously into regions accessible to lasers.

Our measurement is the most stringent experimental test of time dilation, one of the three fundamental concepts of special relativity. Within the RMS framework, this result constrains the existence of a preferred reference frame in the universe (for example, the cosmic-microwave-background frame).

Furthermore, the experiment has been analysed in the context of CPT- and Lorentz-violating extensions of the standard model,

putting unique constraints on some of the parameters^{15,31,32}. In the photon sector, our experiment sets the limit

$$\tilde{\kappa}_{\text{tr}} \lesssim 8.4 \times 10^{-8}.$$

Using the measurements with circularly polarized light, it seems possible to set limits on further, so far unconstrained parameters in the particle sector, and work in this direction is in progress. We also provide the only test of time dilation more sensitive than that derived from the global positioning system^{2,30}.

To conclude, it is interesting to note that the measurement of a single atomic transition to high precision with a fast beam has relevance in relativity, cosmology, particle physics and quantum electrodynamics.

Received 27 June 2007; accepted 1 October 2007; published 11 November 2007.

References

- Einstein, A. Zur Elektrodynamik bewegter Körper. *Ann. Phys.* **322**, 891–921 (1905).
- Ashby, N. Relativity in the global positioning system. *Living Rev. Relativity* **6**, 1 (2003).
- Reichenbach, H. *Relativitätstheorie und Erkenntnis apriori* (Julius Springer, Berlin, 1920).
- Pauli, W. On the conservation of the lepton charge. *Il Nuovo Cimento* **6**, 204–215 (1957).
- Greenberg, O. W. CPT violation implies violation of Lorentz invariance. *Phys. Rev. Lett.* **89**, 231602 (2002).
- Kosteletcký, V. A. & Samuel, S. Spontaneous breaking of Lorentz symmetry in string theory. *Phys. Rev. D* **39**, 683–685 (1989).
- Amelino-Camelia, G., Ellis, J., Mavromatos, N. E., Nanopoulos, D. V. & Sarkar, S. Tests of quantum gravity from observations of gamma-ray bursts. *Nature* **393**, 763–765 (1998).
- Gambini, R. & Pullin, J. Nonstandard optics from quantum space-time. *Phys. Rev. D* **59**, 124021 (1999).
- Einstein, A. Über die Möglichkeit einer neuen Prüfung des Relativitätsprinzips. *Ann. Phys.* **328**, 197–198 (1907).
- Ives, H. E. & Stilwell, G. R. An experimental study of the rate of a moving atomic clock. *J. Opt. Soc. Am.* **28**, 215–226 (1938).
- Lämmerzahl, C. Special relativity and Lorentz invariance. *Ann. Phys.* **14**, 71–102 (2005).
- Mattigling, D. Modern tests of Lorentz invariance. *Living Rev. Relativity* **8**, 5 (2005).
- Robertson, H. P. Postulate versus observation in the special theory of relativity. *Rev. Mod. Phys.* **21**, 378–382 (1949).
- Mansouri, R. & Sexl, R. U. A test theory of special relativity: III. Second-order tests. *Gen. Rel. Grav.* **8**, 809–814 (1977).
- Stanwix, P. L., Tobar, M. E., Wolf, P., Locke, C. R. & Ivanov, E. N. Improved test of Lorentz invariance in electrostatics using rotating cryogenic sapphire oscillators. *Phys. Rev. D* **74**, 081101 (2006).
- Wolf, P. *et al.* Whispering gallery resonators and tests of Lorentz invariance. *Gen. Rel. Grav.* **36**, 2351–2372 (2004).
- Will, C. M. Clock synchronization and isotropy of the one-way speed of light. *Phys. Rev. D* **45**, 403–411 (1992).
- Kretschmar, M. Doppler spectroscopy on relativistic particle beams in the light of a test theory of special relativity. *Z. Phys. A* **342**, 463–469 (1992).
- Amelino-Camelia, G. Special treatment. *Nature* **418**, 34–35 (2002).
- Snyder, J. J. & Hall, J. L. in *Lecture Notes in Physics* Vol. 43 (ed. Haroche, S. *et al.*) (Springer, New York, 1975).
- McGowan, R. W., Giltner, D. M., Sternberg, S. J. & Lee, S. A. New measurement of the relativistic Doppler shift in neon. *Phys. Rev. Lett.* **70**, 251–254 (1993).
- Gwinner, G. Experimental tests of time dilation in special relativity. *Mod. Phys. Lett. A* **20**, 791–805 (2005).
- Riis, E. *et al.* Lamb shifts and hyperfine structure in ${}^6\text{Li}^+$ and ${}^7\text{Li}^+$: Theory and experiment. *Phys. Rev. A* **49**, 207–220 (1994).
- Saathoff, G. *et al.* Improved test of time dilation in special relativity. *Phys. Rev. Lett.* **91**, 190403 (2003).
- Rong, H., Grafström, S., Kowalski, J., Neumann, R. & zu Putlitz, G. A new precise value of the absolute $2\,{}^3S_1, F=5/2 - 2\,{}^3P_2, F=7/2$ transition frequency in ${}^7\text{Li}^+$. *Eur. Phys. J. D* **3**, 217–222 (1998).
- Udem, Th., Holzwarth, R. & Hänsch, T. W. Optical frequency metrology. *Nature* **416**, 233–237 (2002).
- Reinhardt, S. *et al.* Iodine hyperfine structure and absolute frequency measurements at 565, 576, and 585 nm. *Opt. Commun.* **261**, 282–290 (2006).
- Artomi, M., Carusotto, I. & Minardi, F. Light-force-induced fluorescence line-center shifts in high-precision optical spectroscopy: Simple model and experiment. *Phys. Rev. A* **62**, 023402 (2000).
- Riis, E. *et al.* Test of the isotropy of the speed of light using fast-beam laser spectroscopy. *Phys. Rev. Lett.* **60**, 81–84 (1988).
- Wolf, P. & Petit, G. Satellite test of special relativity using the global positioning system. *Phys. Rev. A* **56**, 4405–4409 (1997).
- Hohensee, M., Glenday, A., Li, C.-H., Tobar, M. E. & Wolf, P. Erratum: New methods of testing Lorentz violation in electrodynamics. *Phys. Rev. D* **75**, 049902 (2007).
- Lane, C. D. Probing Lorentz violation with Doppler-shift experiments. *Phys. Rev. D* **72**, 016005 (2005).

Acknowledgements

Technical support from M. Grieser, K. Horn and H. Krieger is gratefully acknowledged. Correspondence and requests for materials should be addressed to G.G.

Reprints and permission information is available online at <http://npg.nature.com/reprintsandpermissions/>